ADVANCED MATERIALS INTERFACES
Open Access
www.advmatinterfaces.de

Substrate Induced van der Waals Force Effects on the Stability of Violet Phosphorus

*Sarabpreet Singh, Mahdi Ghafariasl, Hsin-Yu Ko, Sampath Gamage, Robert A. DiStasio Jr., Michael Snure, and Yohannes Abate**

Since the first isolation of graphene, the importance of van der Waals (vdW) interactions has become increasingly recognized in the burgeoning field of layered materials. In this work, infrared nanoimaging techniques and theoretical modeling are used to unravel the critical role played by interfacial vdW interactions in governing the stability of violet phosphorus (VP)—a recently rediscovered wide bandgap p-type semiconductor—when exfoliated on different substrates. It is demonstrated that vdW interactions with the underlying substrate can have a profound influence on the stability of exfoliated VP flakes and investigate how these interactions are affected by flake thickness, substrate properties (e.g., substrate hydrophilicity, surface roughness), and the exfoliation process. These findings highlight the key role played by interfacial vdW interactions in governing the stability and physical properties of layered materials, and can be used to guide substrate selection in the preparation and study of this important class of materials.

1. Introduction

In a visionary speech in 1960, Feynman memorably highlighted the significance of the non-covalent forces that dominate materials at the nanometer scale.[1] Of particular importance are the vdW forces[2–9] resulting from correlated electronic fluctuations in matter, which govern the structure and stability of the layered materials found on the center stage of contemporary condensed matter physics. Due to their remarkable versatility, vdW forces make it possible to construct nanostructures ranging from atomically thin 2D materials[10–12] to complex vdW heterostructures,[13] providing us access to countless technological applications.[14–16]

vdW and other related interactions[15,17–23] between such materials and the underlying substrate (typically a non-vdW material) are also quite important and can significantly influence the electrical, mechanical, and optical properties of fabricated devices. While a majority of work has focused on characterizing their effect on electrical/optical properties[20] (and hence device performance), interfacial vdW interactions can also impact the stability of layered materials. In particular, the stability of air-sensitive vdW materials such as phosphorus allotropes[24–28] depends on such interfacial forces, which can influence the interaction of a material with its surrounding environment (i.e., potentially reactive species). Substrate hydrophilicity[29] and the extent of layered material/substrate contact are also influenced by interfacial vdW forces and require careful investigation. Furthermore, these interfacial interactions also depend on the thickness of the layered material; hence, the interfacial interactions in thick/bulk layered materials can be fundamentally different[30] from those observed in their ultra-thin counterparts. To protect these materials from degradation and hence preserve their desired properties/performance, it then becomes necessary to select the right substrate[31] for a given application.

VP is a recently rediscovered layered semiconductor with a large tunable direct bandgap (up to 2.5 eV), intrinsic p-type conductivity, and high mobility.[32,33] As such, VP shows great promise for transistor, emitter, and photodetector applications, and is competitive with other intrinsic p-type layered semiconductors. Many of these, including black phosphorus (BP),[24,25,27,34,35] GeAs, GaTe,[36,37] and GaSe[38,39] are quite unstable under ambient conditions. While BP was regarded as the most stable phosphorus allotrope, VP was recently found to be more resistant to oxidation and thermal decomposition, which makes VP more suitable for ambient applications.[25,40,41]

In this work, we investigate the stability and interaction of exfoliated VP flakes with various substrates (SiO_2, Mica, Au, Si) under long-term exposure to air. Using infrared (IR) nanoimaging techniques and theoretical modeling, we demonstrate that vdW

S. Singh, M. Ghafariasl, S. Gamage, Y. Abate
Department of Physics and Astronomy
University of Georgia
Athens, GA 30602, USA
E-mail: yohannes.abate@uga.edu
H.-Y. Ko, R. A. DiStasio Jr.
Department of Chemistry and Chemical Biology
Cornell University
Ithaca, NY 14853, USA
M. Snure
Air Force Research Laboratory
Sensors Directorate
Wright Patterson Air Force Base, Dayton, OH 45433, USA

The ORCID identification number(s) for the author(s) of this article can be found under https://doi.org/10.1002/admi.202400326

DOI: 10.1002/admi.202400326

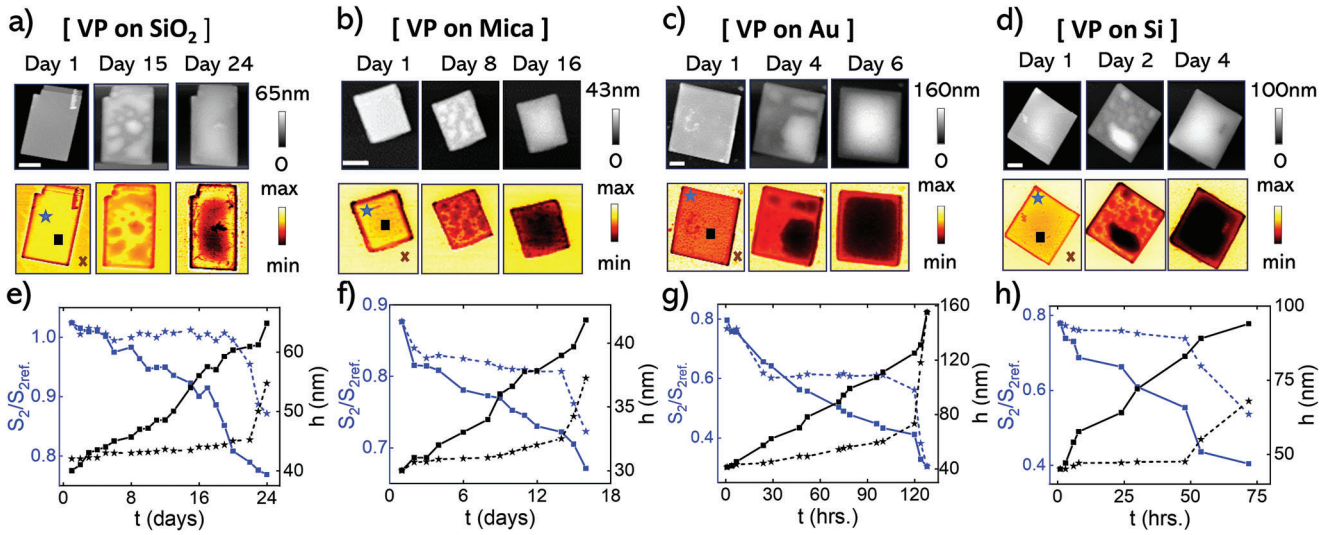

Figure 1. Substrate influence on the stability of exfoliated VP flakes. (a–d) Topography (top panels) and 2nd harmonic IR amplitude images (lower panels) of VP flakes shown for three different days on SiO_2 (thickness ≈41 nm), Mica (thickness ≈30 nm), Au (thickness ≈40 nm), and Si (thickness ≈45 nm) substrates, respectively. (e–h) Topographic heights (black solid and broken lines) and 2nd harmonic normalized amplitudes (blue solid and broken lines) measurements were taken as a function of time; at two different points marked in the Day 1 amplitude images in (a–d). Each normalized point on the near-field amplitude line profile plot was acquired by taking signal at the marked locations normalized by a reference signal on the substrate marked x in the Day 1 amplitude images. Scale bars in the Day 1 topography images (a–d) correspond to 500 nm.

interactions with the underlying substrate can have a profound influence on VP stability; for flakes of similar thicknesses, VP was found to be most stable when exfoliated on a SiO_2 substrate, followed by Mica, Au, and Si. We also investigate how these interactions are affected by the substrate properties and exfoliation process, finding that substrate hydrophobicity and the extent of VP/substrate contact can also influence VP stability. The results of this study highlight the key role played by interfacial vdW interactions in governing the stability and physical properties of layered materials, and can be used to guide substrate selection in the preparation and study of this important class of materials.

2. Results and Discussion

Interactions at the interface between vdW materials and the substrate[42] on which they are exfoliated play a significant role in modifying the intrinsic physical properties of layered materials. Here, we investigate the interplay between exfoliated VP flakes and several substrates using IR nanoimaging (see Experimental Section). **Figure 1** shows the experimental topographic and near-field amplitude measurements of exfoliated VP flakes over an extended time on four different substrates (SiO_2, Mica, Au, and Si). The four substrates were identically prepared and VP flakes of comparable thickness were exfoliated on them. The thickness of the flakes was kept in the range of ≈30–45 nm and all flakes on each substrate were consecutively measured using IR nanoimaging keeping all experimental conditions identical. Both the topography and near-field amplitude images and line profiles from a VP flake on SiO_2 (Figure 1a,e) show slow changes over a 24-day period, which is also shown in the topographic height (black solid and broken lines) and 2nd harmonic normalized amplitude (blue solid and broken lines) taken at two different points on the sample marked in the amplitude image in Figure 1a; see Figure S2 (Supporting Information) for topography and near-field measurements for all consecutive days. Data from two different points are presented to capture the non-uniformity of the VP surface modification over time. When we perform similar experiments on a 30 nm thick VP flake exfoliated on a Mica substrate under the same experimental conditions, we observe faster oxidation (16 days for complete surface degradation) as indicated by the changes in the topography and near-field amplitude images and line profiles shown in Figure 1b,f (Figure S3, Supporting Information shows measurements for all days). On Au (Figure 1c,g and S4, Supporting Information), VP (thickness ≈40 nm) completely degrades in 6 days, resulting in a ≈100 nm topographic height increase and a corresponding decrease in the normalized near-field amplitude. On Si, VP (≈45 nm) oxidizes the fastest, completely oxidizing in 4 days with a topographic height increase of ≈50 nm and a steep decrease in the normalized amplitude signal. Both an increase in the topographic height and a decrease in the time-dependent near-field normalized amplitude signal are hallmarks of degradation as previously reported.[24–27,43–47] The near-field amplitude decrease over time in Figure 1e–h is because the IR photons directly probe the changing permittivity of the sample due to degradation. To confirm the formation of oxidized phosphorus species on VP exfoliated on different substrates, we also conducted nano-spectroscopy over time, and the resulting spectra and assignments are shown in Figure S6 (Supporting Information). These experimental results show that VP is stable for longer times under ambient conditions when prepared on a SiO_2 substrate, followed by Mica, Au, and Si. Additional measurements and analysis for exfoliated VP flakes with similar thicknesses confirm these trends (see Figure S9, Supporting Information).

We note, however, that in the ultra-thin thickness regime, the stability and interaction of layered materials with the

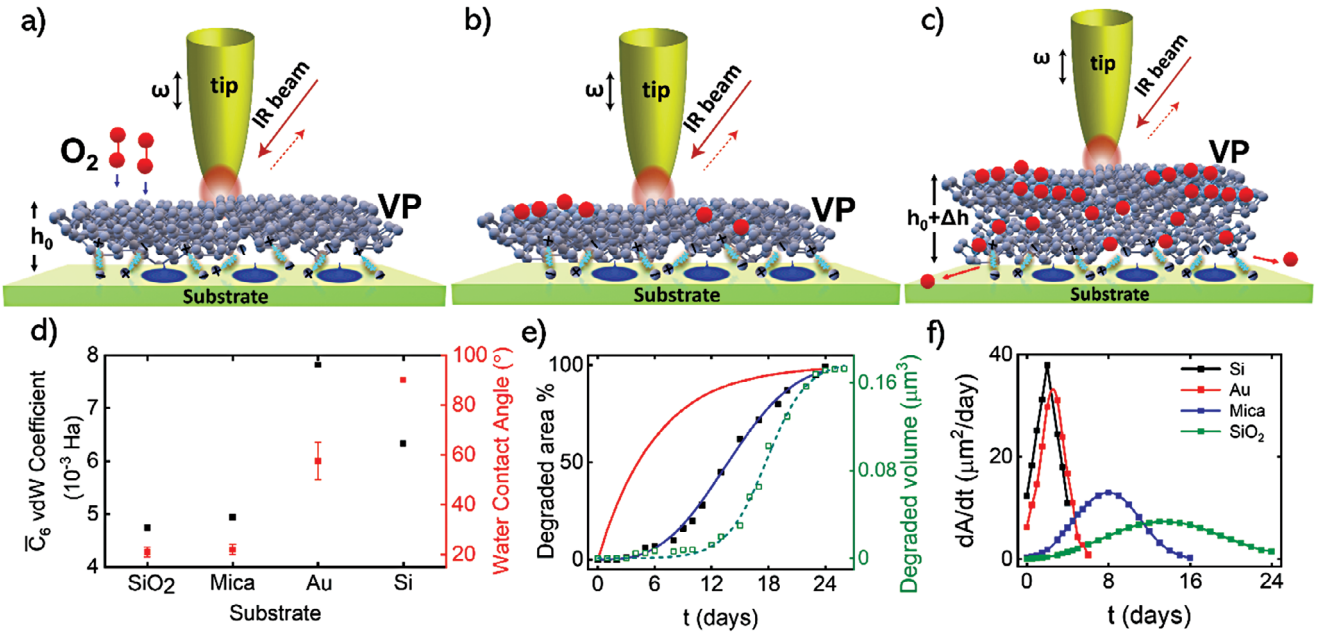

Figure 2. Influence of VP-substrate vdW interactions and substrate hydrophilicity on VP stability. (a–c) Schematic showing the interaction of VP with O_2 molecules. (d) VP-substrate vdW coefficients (see Supporting Information for more details) and water contact angles for the SiO_2, Mica, Au, and Si substrates. (e) Experimental (black squares) and simulated (blue and red curves, obtained using a forest fire model, see Supporting Information) degraded area percentages as a function of time for VP exfoliated on SiO_2. Also plotted are the experimental (green open squares) volumes of the degraded bubble as a function of time as well as a sigmoidal fit to the experimental data (dashed green line). (f) Plot of the slope of the degraded area (dA/dt) as a function of time for VP exfoliated on all four substrates.

substrate can be fundamentally different from those in the thickness range considered in this work.[30] The interactions observed in bulk (i.e., thick vdW layers) represent a fundamentally different regime, given the pronounced differences in the interfacial vdW forces and surface-to-volume ratio compared to ultra-thin counterparts. In Figure S1 (Supporting Information), we present a case study where thinner VP flakes degrade within 4 days even on a SiO_2 substrate, which is considerably faster than that observed for thicker flakes (Figure 1). Since the current work focuses on flakes with thicknesses greater than 30 nm, the insights and conclusions drawn below may not be applicable to VP flakes below this thickness range.

The influence of the substrate on the stability of VP in Figure 1 is sizeable and quite interesting. Since the top surfaces of the exfoliated VP flakes in this work (all of which have thicknesses ≥30 nm) are far from the substrate, one might assume that the interactions between VP and the environment (i.e., that lead to degradation) would be indifferent to the VP-substrate interfacial vdW forces. To explain these peculiar observations, we considered two potentially distinguishing characteristics of the underlying substrates: (1) the strength of the VP-substrate vdW interactions; and (2) the hydrophilicity/hydrophobicity of the substrates. To quantify the relative strength of the vdW interactions between VP and the four substrates considered herein, we performed a series of first-principles electronic structure calculations to compute the VP-substrate vdW coefficients. To quantify the hydrophilicity/hydrophobicity effect, we compared experimentally determined water contact angles (WCA) for each substrate. Based on these two characteristics, we propose mechanism below to explain the observed substrate-dependent stability of thick exfoliated VP flakes. A schematic depicting the surface topographic changes and chemical modifications that occur during the VP degradation process is provided in **Figure 2a–c**. As soon as VP is exfoliated on a substrate, it begins to interact with potential reactants (i.e., O_2 and H_2O)[48] in the atmosphere (Figure 2a). The top surface of the VP flake then undergoes a series of chemical reactions (Figure 2b), which leads to topographic height changes and the formation of phosphorus oxide (PO_x) species. The degradation process continues down as these reactive species diffuse into sub-layers of the VP flake (Figure 2c) via cracks formed during degradation (see Figure S10, Supporting Information for a STEM image showing the formation of a hole during degradation). This leads to an increase in the VP flake height combined with a decrease in the IR optical constant (as probed by the IR nanoimaging tip).

In our proposed mechanism, interfacial VP-substrate vdW interactions can influence the degradation process by altering the porosity of thick exfoliated VP flakes and hence guest-molecule dwell times. More specifically, VP-substrate combinations with relatively weak interfacial vdW interactions will tend to increase the porosity and decrease the guest-molecule dwell times in the exfoliated VP flake, thereby opening pathways for potential reactants (and other intermediates) to diffuse away. In doing so, the substrate influence would slow down the degradation process. To quantify the relative strength of the vdW interactions between VP and the four substrates above, VP-substrate vdW coefficients ($\bar{C}_{6,\mathrm{VP-sub}}$) were obtained using first-principles electronic structure calculations (see Supporting Information).[49–54]

As shown in Figure 2d, the theoretical $\bar{C}_{6,\mathrm{VP-sub}}$ vdW coefficients correlate quite well with our experimental observations

regarding the stability of VP exfoliated on different substrates: the VP-substrate combinations with comparatively weaker vdW interactions (i.e., VP-SiO_2 and VP-Mica) have the slowest degradation rates, while those with stronger vdW interactions (i.e., VP-Au and VP-Si) degrade much faster (see Figure 1). Here, we note that the order of VP-Au and VP-Si are inverted with respect to the observed degradation rates, and attribute this difference (at least in part) to potential variations in the Au surface (e.g., oxidation, surface irregularities, trace amounts of adventitious carbon) which can have non-negligible effects on the strength of the VP-substrate vdW interactions; for instance, we estimate that the $\bar{C}_{6,\mathrm{VP-sub}}$ coefficient could be reduced by ≈10% upon oxidation of Au to Au_2O_3. Nevertheless, our theoretical ranking of these interaction strengths provides a first pillar of support for the critical role played by VP-substrate vdW interactions in the VP degradation process.

As a second distinguishing characteristic among these substrates, we also considered how the hydrophilicity of the substrate could influence the stability of thick exfoliated VP flakes. Here, we would argue that the more hydrophilic substrates will have an increased tendency to attract water to their surfaces, which can screen/weaken the interfacial VP-substrate vdW interactions as well as re-route water away from competing hydrophilic PO_x sites in the VP flake—both of these effects would attenuate the substrate-induced degradation process and improve VP stability. By considering the experimental water contact angles (WCA) for each substrate (see Figure 2d),[55–60] we find that the degradation rates for thick exfoliated VP flakes are indeed very well-correlated with the WCA values. In other words, the slowest degradation rates were observed for VP flakes exfoliated on the most hydrophilic substrates, i.e., SiO_2 (WCA = 21°)[57–60] and Mica (WCA = 22°).[56] On the other hand, Si is the least hydrophilic (WCA = 90°)[55] substrate and has the fastest degradation rate. Here, we would add that VP flakes exfoliated on Au degrade at an intermediate rate (that is much closer to Si than SiO_2 or Mica), which is consistent with the fact that Au is more hydrophilic than Si, but less hydrophilic than SiO_2 or Mica. While there is some experimental uncertainty in the WCA values for SiO_2 and Mica, the error bars are quite small and not easily discernible in Figure 2d. This is not the case for Au, where it is now accepted that a meticulously clean Au surface is hydrophilic (WCA = 0°), while the presence of a relatively small amount (<1 ML) of adventitious carbon will effectively render the surface hydrophobic (50° < WCA < 65°).[61] Even with the inclusion of such nuances originating from the (albeit more complicated) Au surface, our analysis of substrate hydrophilicity provides a second pillar of support for the critical role played by VP-substrate vdW interactions in governing the stability of VP.

To gain additional insight into the evolution of the VP surface morphology as a function of time due to chemical oxidation, we employed a variant of the forest fire model used in earlier work.[27] This model provides several useful qualitative insights into the surface morphological modification process. This model is based on a simple probabilistic description of the sample surface, which is divided into $N \times N$ square elements, with each element in a degraded or undegraded state. The function $P_n = 1 - \exp[-\Delta t \cdot \eta^{(n)}]$ gives the degradation probability after a time interval Δt, in which the degradation probability per unit time is given by $\eta^{(n)}$ with n degraded neighbors (here, $0 \leq n \leq 8$) is merely a fitting parameter. $\Delta\eta$ is the fixed increase in each degraded neighbor and can be written as $\eta^{(n)} = \eta^{(0)} + n\Delta\eta$, where $\eta^{(0)}$ is the degradation probability per unit time if all neighbors are undegraded. This model provides several useful qualitative insights into the surface morphological modification process. As an example, we plot the experimental degradation area percentage (black solid squares) and volume (green open squares) as a function of time for VP on SiO_2 in Figure 2e (we note that the trend is similar for the other substrates, see Figures S7 and S8in the Supporting Information). The blue line shows a fit of the degradation area percentage using the forest fire model including neighboring interactions, while the red line shows a fit of the degradation area percentage using the forest fire model without the neighboring interactions. To fit the percentage volume of the degraded region (open green squares), we used the well-known sigmoidal growth curve (green line). We found a good fit with the experimental degraded surface area results using $\eta^{(0)} = 0.015\mathrm{d}^{-1}$ and $\Delta\eta = 1.65\mathrm{d}^{-1}$. The red line shows a fitting, with all parameters kept the same, but without including neighboring interactions ($\Delta\eta = 0$). It is clear from Figure 2e that the experimental data fits better when we consider neighboring interactions. This can be explained by invoking a diffusion model (schematics shown in Figure 2a–c). As oxygen diffuses into the VP layer, it collides with phosphorous atoms and if the phosphorus atoms are still unreacted and available it has a higher probability of interacting. If on the other hand, the phosphorous atoms are all reacted, the oxygen will simply bounce off and move to the next neighboring phosphorus. In this way, a "degraded/reacted" phosphorus makes it more probable for an undegraded region of the flake to degrade (i.e., neighbors matter). The comparison between the sigmoidal growth curve (green curve) for the volume change and the simulated degraded area percentages with neighboring interactions (blue curve) seems to indicate that surface degradation happens more quickly than volume deformation. To show the difference in the degradation rate of VP on different substrates, we find it more instructive to plot the slope of the degraded area as a function of time (dA/dt vs t) as shown in Figure 2f. This plot shows a Gaussian distribution for VP exfoliated on Si, Mica, and Au substrates, where the largest maximum slope (dA/dt) means VP degrades the fastest. VP on Mica shows the second slowest degradation next to VP on the SiO_2 substrate.

We further investigated the influence of interfacial vdW interactions on VP degradation by preparing two flakes of similar thicknesses (64 and 67 nm) on two Si substrates that were etched to produce different surface roughnesses as a way to reduce the VP-substrate vdW interaction (**Figure** 3d,e). We compare the degradation of these two samples to a suspended VP flake surrounded by air that does not interact with a substrate (Figure 3f). The VP on the smooth (3 nm roughness) Si substrate shows a rapid increase in topographic height from 64 nm to 160 nm and a linear decrease in normalized amplitudes over four days as shown in Figure 3g. Figure 3e shows data from a 67 nm VP flake on the rough (22 nm roughness) Si substrate. This flake completely degraded in six days, where the height increased by more than three times (Figure 3h) and the normalized amplitude decreased from 0.60 to 0.40. In the suspended VP flake (94 nm thick), no appreciable change in the topographic height or normalized amplitude was observed over 15 days (Figure 3i). On the smooth Si substrate with the largest VP-substrate vdW

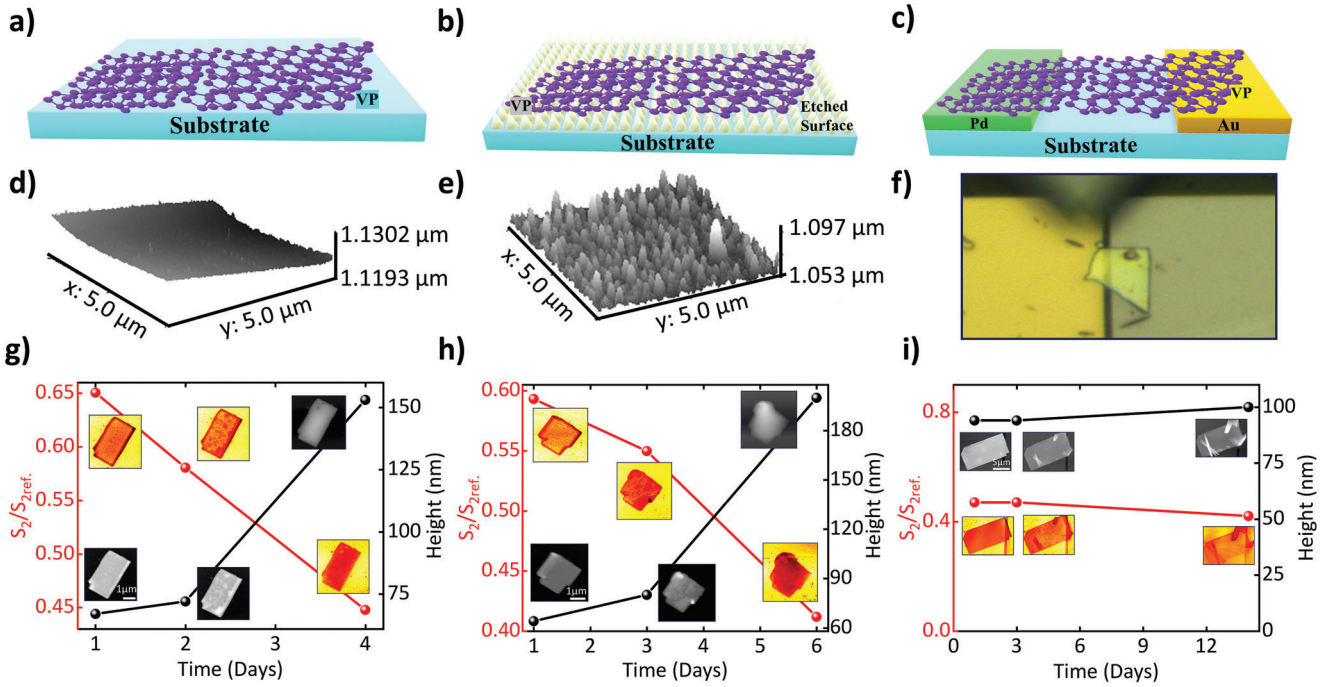

Figure 3. Influence of VP-substrate contact area on VP stability Depiction of a VP flake exfoliated (a) on a Si substrate etched for less than 1 s, (b) on a 600 s etched Si substrate, and (c) a suspended VP flake. (d,e) 3D topographic images of <1 s and 600 s etched Si substrates, respectively. To produce Si substrates with different surface roughnesses, we etched the surface of a Si substrate as shown in Figure 3e using a buffered oxide etch solution comprised of 40% NH_4F in water and 49% HF in water in a ratio of 6:1 for either less than 1 s or 600 s, resulting in roughness values of 3 nm and 22 nm, before exfoliating VP. (f) Optical image of a VP flake over the gap between two electrodes. (g–i) Variation of height and normalized second harmonic amplitude with time along with the images of VP topography and second harmonic amplitude on <1 sec etched Si substrate, 600 sec etched Si substrate, and the suspended flake.

interactions VP degrades the fastest, while the suspended flake with the least VP-substrate vdW interactions experience the slowest degradation. The flake on the rough Si substrate (intermediate VP-substrate vdW interactions) shows a degradation time between these two cases. These experiments highlight the dependence of the degradation process on the interfacial vdW interactions between the exfoliated VP flake and the substrate, an effect that also needs tobe considered in device/sample manufacturing.

Finally, we compare the degradation of VP exfoliated on Mica in air and nitrogen environments, as well as the effect of heating the Mica substrate prior to exfoliation (Figure 1b,f). To isolate the effects of air during the exfoliation process, we used a nitrogen glove box and prepared a VP sample under deoxygenated low-humidity conditions. We first exfoliated VP in a nitrogen environment without heating the Mica substrate (**Figure 4a**) and brought the sample out of the glove box for SNOM measurements in

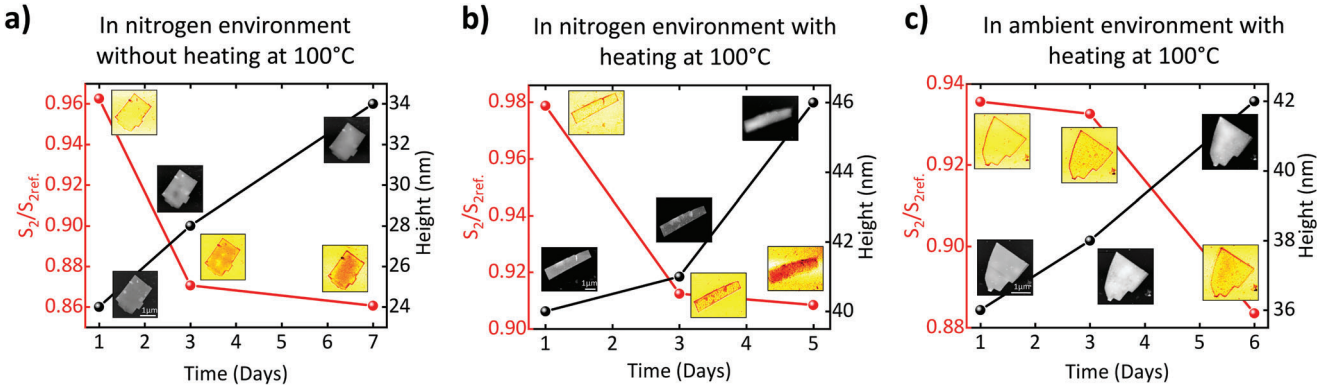

Figure 4. Influence of oxygenated and deoxygenated environments on the stability of VP exfoliated on Mica. Variation of the normalized second harmonic amplitude and height over time (days) for VP flakes exfoliated (a) in a nitrogen glove box with no substrate heating, (b) in a nitrogen glove box after heating the substrate to 100 °C, and (c) in air after heating the substrate to 100 °C. Topography and second harmonic amplitude images taken with IR scattering type scanning near-field microscope (s-SNOM) at a frequency of 952 cm^{-1} are shown in the insets.

the ambient environment. This results in the degradation of VP within 7 days of exfoliation since the sample is exposed to oxygen and water. We then prepared a second sample in the glove box where the Mica substrate was heated to 100 °C for 2–3 min then cooled, followed by exfoliation of VP (Figure 4b). Again, although the flake was prepared in a nitrogen glove box, measurements were taken in ambient conditions, it still degraded completely within five days. To further compare the effects of the substrate conditions, Mica was heated to 100 °C in ambient conditions and then cooled to room temperature (Figure 4c) followed by exfoliation of a VP flake. In this case, the sample degraded completely in 6 days. These results show that heating the Mica substrate or placing it in a deoxygenated environment increases the pace of degradation. We suspect that heating the Mica before VP exfoliation causes it to lose water, altering its hydrophilic properties.[62,63]

3. Conclusions

In this work, we investigated the effect of interfacial vdW interactions and hydrophobicity of various substrates on the chemical stability of exfoliated VP flakes using nanoscale IR imaging techniques and theoretical modeling. A detailed comparison of four substrates clearly showed that VP flakes (30 nm or more) exfoliated on SiO_2 to be the most stable followed by VP flakes exfoliated on Mica, Au, and Si. We find that the strength of the interfacial vdW interactions and the hydrophobicity/hydrophilicity of the substrate play a key role in the degradation of VP and can extend the lifetime by more than three times. By modifying surface roughness, we further show the impact that VP-substrate vdW interactions have on the VP degradation process. Whereas VP on a smooth Si substrate, which has stronger vdW interactions, leads to faster degradation. Additionally, we examined the effects of oxygen and substrate heating during exfoliation on VP degradation. We note that the interactions between vdW materials and their substrates is very complex, involving multi-electron interactions, electronic energy level alignment, and chemical complexities, among other factors, which were not explored in the current study.[64] Consequently, our research could set the stage for more detailed investigations into interface physics.

4. Experimental Section

Material Synthesis: Violet phosphorus (VP) flakes were mechanically exfoliated from bulk samples obtained from HQ Graphene, which were produced by chemical vapor transport, using adhesive tape. Exfoliated flakes were then transferred onto different substrates for characterization. The humidity in the lab was regulated to remain below 50% for the experiments. The samples were consistently exposed to ambient conditions and were stored underroom temperature conditions for the duration of the experiments. The oxygen level was < 1 ppm in the glove box for the exfoliation of VP flakes in the deoxygenated environment.

IR Nanoimaging: Topographic and IR nanoimaging of VP flakes were performed using a commercial IR scattering-type scanning near-field microscope (s-SNOM)[65] from Attocube co. s-SNOM was based on a tapping mode AFM equipped with a cantilevered metal-coated tip. The tip oscillates at a resonance frequency $\Omega \approx 270$ kHz and a tapping amplitude of ≈100 nm. An IR quantum cascade laser ($\lambda = 10.5$ µm) was focused by a parabolic mirror onto the metalized tip and interacts with the sample. The scattered light from the tip-sample junction was demodulated at the second harmonics of the tip resonance frequency (2 Ω) and detected by phase modulation (pseudo-heterodyne) interferometry, resulting in simultaneous topography, optical amplitude, and phase images. s-SNOM provides material contrast imaging with a spatial resolution down to ≈10 nm independent of the incident wavelength used from visible to terahertz frequency range.[66]

STEM: VP flakes were prepared through a liquid-phase exfoliation technique for STEM measurements. Initially, sonication was carried out in 2-propanol for a duration of 60 min to prepare these flakes. Subsequently, this VP-infused solvent was applied to a TEM grid by the drop casting-method and left to dry for 1 h. Once the solution dried on the grid, STEM images of the VP flake were captured at a 30-kilovolt acceleration voltage using an SU-9000 system. Images were taken on the VP flake at high magnification on the 1st, 3rd, and 7th-days post preparation.

Supporting Information

Supporting Information is available from the Wiley Online Library or from the author.

Acknowledgements

Support for the works of S.S., S.G., and Y.A. was provided by the Air Force Office of Scientific Research (AFOSR) grant numbers FA9550-19-0252 and FA9550-23-1-0375. M.S. acknowledges funding from the Air Force Office of Scientific Research under Award No. FA9550-24RYCOR011. M.G. acknowledges support from the Gordon and Betty Moore Foundation, GBMF12246 and grant DOI 10.37807/GBMF12246. R.A.D. and H.-Y.K. acknowledge funding from the National Science Foundation under Grant No. CHE-1945676. R.A.D. also gratefully acknowledges financial support from an Alfred P. Sloan Research Fellowship. This research used resources of the National Energy Research Scientific Computing Center, which is supported by the Office of Science of the U.S. Department of Energy under Contract No. DE-AC02-05CH11231. [Correction added on July 24, 2024, after first online publication: The supporting file has been updated in this version.]

Conflict of Interest

The authors declare no conflict of interest.

Data Availability Statement

The data that support the findings of this study are available from the corresponding author upon reasonable request.

Keywords

degradation, hydrophilicity, infrared imaging, van der Waals interactions, violet phosphorus

Received: April 18, 2024
Revised: June 18, 2024
Published online: July 1, 2024

[1] R. P. Feynman, *J. Microelectromech. Syst.* **1992**, *1*, 60.
[2] A. Tkatchenko, *Adv. Funct. Mater.* **2015**, *25*, 2054.
[3] V. A. Parsegian, *Van der Waals Forces: A Handbook for Biologists, Chemists, Engineers, and Physicists*, Cambridge University Press, Cambridge, United Kingdom, **2005**.

[4] R. H. French, V. A. Parsegian, R. Podgornik, R. F. Rajter, A. Jagota, J. Luo, D. Asthagiri, M. K. Chaudhury, Y.-m. Chiang, S. Granick, *Rev. Mod. Phys.* **2010**, *82*, 1887.
[5] D. Langbein, *Springer Tracts in Modern Physics*, Springer, Berlin, Heidelberg, **1974**, https://doi.org/10.1007/BFb0042407.
[6] I. E. Dzyaloshinskii, E. M. Lifshitz, L. P. Pitaevskii, *Adv. Phys.* **1961**, *10*, 165.
[7] J. Hermann, R. A. DiStasio Jr., A. Tkatchenko, *Chem. Rev.* **2017**, *117*, 4714.
[8] A. Ambrosetti, N. Ferri, R. A. DiStasio Jr., A. Tkatchenko, *Science* **2016**, *351*, 1171.
[9] Y. Yang, K. U. Lao, R. A. DiStasio Jr., *Phys. Rev. Lett.* **2019**, *122*, 026001.
[10] K. Novoselov, A. Mishchenko, A. Carvalho, A. Castro Neto, *Science* **2016**, *353*, aac9439.
[11] A. K. Geim, K. S. Novoselov, *Nat. Mater.* **2007**, *6*, 183.
[12] Z. Lu, M. L. Dunn, *J. Appl. Phys.* **2010**, *107*, 044301.
[13] A. K. Geim, I. V. Grigorieva, *Nature* **2013**, *499*, 419.
[14] R. Lv, J. A. Robinson, R. E. Schaak, D. Sun, Y. Sun, T. E. Mallouk, M. Terrones, *Acc. Chem. Res.* **2015**, *48*, 56.
[15] S. M. Auerbach, K. A. Carrado, P. K. Dutta, *Handbook of Layered Materials*, CRC Press, Boca Raton, **2004**.
[16] D. L. Duong, S. J. Yun, Y. H. Lee, *ACS Nano* **2017**, *11*, 11803.
[17] M. Rösner, E. Şaşıoğlu, C. Friedrich, S. Blügel, T. Wehling, *Phys. Rev. B* **2015**, *92*, 085102.
[18] R. T. Cygan, J. A. Greathouse, H. Heinz, A. G. Kalinichev, *J. Mater. Chem.* **2009**, *19*, 2470.
[19] N. Marom, J. Bernstein, J. Garel, A. Tkatchenko, E. Joselevich, L. Kronik, O. Hod, *Phys. Rev. Lett.* **2010**, *105*, 046801.
[20] M.-Y. Li, C.-H. Chen, Y. Shi, L.-J. Li, *Mater. Today* **2016**, *19*, 322.
[21] X. Zhou, X. Hu, J. Yu, S. Liu, Z. Shu, Q. Zhang, H. Li, Y. Ma, H. Xu, T. Zhai, *Adv. Funct. Mater.* **2018**, *28*, 1706587.
[22] A. Fali, T. Zhang, J. P. Terry, E. Kahn, K. Fujisawa, B. Kabius, S. Koirala, Y. Ghafouri, D. Zhou, W. Song, *ACS Nano* **2021**, *15*, 2447.
[23] S. Xie, L. Tu, Y. Han, L. Huang, K. Kang, K. U. Lao, P. Poddar, C. Park, D. A. Muller, R. A. DiStasio Jr., J. Park, *Science* **2018**, *359*, 1131.
[24] Y. Abate, S. Gamage, Z. Li, V. Babicheva, M. H. Javani, H. Wang, S. B. Cronin, M. I. Stockman, *Light Sci. Appl.* **2016**, *5*, e16162.
[25] A. Fali, M. Snure, Y. Abate, *Appl. Phys. Lett.* **2021**, *118*, 163105.
[26] S. Gamage, A. Fali, N. Aghamiri, L. Yang, P. D. Ye, Y. Abate, *Nanotechnology* **2017**, *28*, 265201.
[27] S. Gamage, Z. Li, V. S. Yakovlev, C. Lewis, H. Wang, S. B. Cronin, Y. Abate, *Adv. Mater. Interfaces* **2016**, *3*, 1600121.
[28] L. Peng, N. Abbasi, Y. Xiao, Z. J. Xie, *Adv. Mater. Interfaces* **2020**, *7*, 23.
[29] J. D. Wood, S. A. Wells, D. Jariwala, K.-S. Chen, E. Cho, V. K. Sangwan, X. Liu, L. J. Lauhon, T. J. Marks, M. C. Hersam, *Nano Lett.* **2014**, *14*, 6964.
[30] Y. He, W. Chen, W. Yu, G. Ouyang, G. Yang, *Sci. Rep.* **2013**, *3*, 2660.
[31] A. J. Mannix, B. Kiraly, M. C. Hersam, N. P. Guisinger, *Nature Rev. Chem.* **2017**, *1*, 0014.
[32] G. Schusteritsch, M. Uhrin, C. J. Pickard, *Nano Lett.* **2016**, *16*, 2975.
[33] A. G. Ricciardulli, Y. Wang, S. Yang, P. Samori, *J. Am. Chem. Soc.* **2022**, *144*, 3660.
[34] J. O. Island, G. A. Steele, H. S. van der Zant, A. Castellanos-Gomez, *2D Mater.* **2015**, *2*, 011002.
[35] Y. Abate, D. Akinwande, S. Gamage, H. Wang, M. Snure, N. Poudel, S. B. Cronin, *Adv. Mater.* **2018**, *30*, 1704749.
[36] E. Zallo, A. Pianetti, A. S. Prikhodko, S. Cecchi, Y. S. Zaytseva, A. Giuliani, M. Kremser, N. I. Borgardt, J. J. Finley, F. Arciprete, *NPJ 2D Mater. Appl.* **2023**, *7*, 19.
[37] E. Mercado, Y. Zhou, Y. Xie, Q. Zhao, H. Cai, B. Chen, W. Jie, S. Tongay, T. Wang, M. Kuball, *ACS Omega* **2019**, *4*, 18002.
[38] M. Yagmurcukardes, R. T. Senger, F. M. Peeters, H. Sahin, *Phys. Rev. B* **2016**, *94*, 245407.
[39] A. Bergeron, J. Ibrahim, R. Leonelli, S. Francoeur, *Appl. Phys. Lett.* **2017**, *110*, 241901.
[40] L. Zhang, H. Huang, B. Zhang, M. Gu, D. Zhao, X. Zhao, L. Li, J. Zhou, K. Wu, Y. Cheng, *Angew. Chem.* **2020**, *132*, 1090.
[41] M. Ghafariasl, S. Singh, S. Gamage, T. Prusnick, M. Snure, Y. Abate, *Adv. Mater. Interfaces* **2024**, *11*, 2300794.
[42] R. Bian, C. Li, Q. Liu, G. Cao, Q. Fu, P. Meng, J. Zhou, F. Liu, Z. Liu, *Natl. Sci. Rev.* **2022**, *9*, nwab164.
[43] Y. Abate, D. Akinwande, S. Gamage, H. Wang, M. Snure, N. Poudel, S. B. Cronin, *Adv. Mater.* **2018**, *30*, 1704749.
[44] J. Xue, S. Wang, J. Zhou, Q. Li, Z. Zhou, Q. Hui, Y. Hu, Z. Zhou, Z. Feng, Q. Yan, *Appl. Phys. Lett.* **2023**, *122*, 181903.
[45] T. Zhang, Y. Wan, H. Xie, Y. Mu, P. Du, D. Wang, X. Wu, H. Ji, L. Wan, *J. Am. Chem. Soc.* **2018**, *140*, 7561.
[46] W. Luo, D. Y. Zemlyanov, C. A. Milligan, Y. Du, L. Yang, Y. Wu, D. Y. Peide, *Nanotechnology* **2016**, *27*, 434002.
[47] S. Wu, F. He, G. Xie, Z. Bian, J. Luo, S. Wen, *Nano Lett.* **2018**, *18*, 5618.
[48] Y. Huang, J. Qiao, K. He, S. Bliznakov, E. Sutter, X. Chen, D. Luo, F. Meng, D. Su, J. Decker, *Chem. Mater.* **2016**, *28*, 8330.
[49] V. Blum, R. Gehrke, F. Hanke, P. Havu, V. Havu, X. Ren, K. Reuter, M. Scheffler, *Comput. Phys. Commun.* **2009**, *180*, 2175.
[50] J. P. Perdew, K. Burke, M. Ernzerhof, *Phys. Rev. Lett.* **1996**, *77*, 3865.
[51] J. Hermann, A. Tkatchenko, *Phys. Rev. Lett.* **2020**, *124*, 146401.
[52] A. Tkatchenko, R. A. DiStasio Jr., R. Car, M. Scheffler, *Phys. Rev. Lett.* **2012**,*108*, 236402.
[53] A. Ambrosetti, A. M. Reilly, R. A. DiStasio Jr., A. Tkatchenko, *J. Chem. Phys.* **2014**, *140*, 18A508.
[54] A. Stone, *The Theory of Intermolecular Forces*, Oxford University Press, Oxford, **2013**.
[55] P. Bryk, E. Korczeniewski, G. S. Szymański, P. Kowalczyk, K. Terpiłowski, A. P. Terzyk, *Materials* **2020**, *13*, 1554.
[56] E. Rossi, P. S. Phani, R. Guillemet, J. Cholet, D. Jussey, W. Oliver, M. Sebastiani, *J. Mater. Res.* **2021**, *36*, 2357.
[57] N. Martinez, *Wettability of Silicon, Silicon Dioxide, and Organosilicate Glass*, University of North Texas, Denton,Texas, **2009**.
[58] C. P. Stallard, K. A. McDonnell, O. D. Onayemi, J. P. O'Gara, D. P. Dowling, *Biointerphases* **2012**, *7*, 31.
[59] R. Frieser, *J. Electrochem. Soc.* **1974**, *121*, 669.
[60] E. K. Kim, J. Y. Kim, S. S. Kim, *Surf. Interface Anal.* **2013**, *45*, 656.
[61] T. Smith, *J. Colloid Interface Sci.* **1980**, *75*, 51.
[62] Z. Li, Y. Wang, A. Kozbial, G. Shenoy, F. Zhou, R. McGinley, P. Ireland, B. Morganstein, A. Kunkel, S. P. Surwade, *Nat. Mater.* **2013**, *12*, 925.
[63] X. Gong, A. Kozbial, L. Li, *Chem. Sci.* **2015**, *6*, 3478.
[64] Z.-F. Liu, F. H. daJornada, S. G. Louie, J. B. Neaton, *J. Chem. Theory Comput.* **2019**, *15*, 4218.
[65] S. Gamage, S. Manna, M. Zajac, S. Hancock, Q. Wang, S. Singh, M. Ghafariasl, K. Yao, T. Tiwald, T. J. Park, *arXiv* **2023**, 230904486.
[66] X. Chen, D. Hu, R. Mescall, G. You, D. Basov, Q. Dai, M. Liu, *Adv. Mater.* **2019**, *31*, 1804774.